Nuclear Electric Field Gradient and Mean-Square Displacement Tensors in Tellurium Metal*

P. Boolchand†, B. L. Robinson‡, and S. Jha†
Case Western Reserve University, Cleveland, Ohio 44106
(Received 6 March 1970)

The Mössbauer effect in Te single-crystal absorbers was studied along different crystal axes. Area ratios of the quadrupole doublet were used as an experimental parameter to extract the electric field gradient and mean-square displacement tensors. Experimental data, taken at the temperature of liquid helium, are well fitted by collinear principal axes for the electric field gradient and mean-square displacement tensors. The quadrupole splitting, asymmetry parameter, and mean-square displacement parameters are $\Delta E_q = 7.74 \pm 0.10$ mm/sec, $\eta = 0.64 \pm 0.04$, $\langle x^2 \rangle = \langle y^2 \rangle = \langle z^2 \rangle = (1.6 \pm 0.05)\,\text{Å}^2$.

I. INTRODUCTION

All stable odd-A Te isotopes have ground-state spin $\frac{1}{2}$; therefore, electric quadrupole interaction studies are possible only by utilizing the excited states. For this reason, Mössbauer-effect (ME) studies in Te^{125} offer a unique tool to study electric hyperfine fields at Te nuclei in different crystalline environments. In particular, for Te metal which is known to possess a rather noncubic crystal structure, [1] large electric field gradients (EFG) have been reported. [2-4] The ME of the 35.5-keV ($\frac{3}{2}^+ \rightarrow \frac{1}{2}^+$; $M1$) transition in Te metal shows a partially resolved doublet. A number of investigations of the quadrupole splitting at different temperatures in polycrystalline absorbers have been reported in the literature. [5,6] A complete description of the EFG parameters in Te metal, however, is not possible from polycrystalline studies alone.

In this paper, we present a systematic study of electric quadrupole interaction and recoil-free fraction in Te metal using, for the first time, single-crystal absorbers. All measurements were made at the temperature of liquid helium. The ME was observed along different crystal axes of Te-metal crystal, and the area ratios of the quadrupole doublet were used as experimental parameters to obtain EFG and mean-square displacement (MSD) parameters. Similar studies using the area-ratio technique have been carried out in single crystals of some iron compounds. [7-10]

II. CRYOSTAT, SOURCE, AND ABSORBERS

The Mössbauer spectrometer consisted of a constant-acceleration electromechanical-drive system with a 400-channel analyzer. A cryogenic assembly provided for source and absorber cooling to liquid-helium temperature. A detailed description of the assembly has been given by Kalvius. [11]

The radioactive source I^{125}, in a Cu matrix, was used as a single-line source of 35.5-keV γ rays. Figure 1 shows a pulse-height spectrum of radiations from this source taken with a Si(Li) detector. The 35.5-keV γ ray appears well resolved from the x rays. It may be pointed out that the 22.5- and 24.8-keV peaks appearing in the spectrum are presumably due to Ag impurity in the source. Owing to the poor efficiency of our Si(Li) detector, most of our Mössbauer studies with Te^{125} were carried out with Xe proportional counter. Figure 2 shows a typical pulse-height spectrum of radiation with the proportional counter. The Mössbauer studies were carried out by utilizing the escape peak of the 35.5-keV γ rays. [3] The dilution due to the Cu x ray was minimized by using Al absorbers of appropriate thickness.

Mössbauer spectra were taken with a number of thin ZnTe absorbers and Fig. 3 shows a typical result. For these measurements, the source and the absorbers were maintained at liquid-nitrogen temperature. From our measurements, we calculate the full width at half-maximum of our source as 5.8 ± 0.1 mm/sec. This value is 12% larger than the expected natural [12] linewidth of 5.2 mm/sec for the 2.15-nsec 35.5-keV state of Te^{125}.

Single-crystal absorbers were prepared by spark cutting thin platelets from a large (2 in. $\times \frac{1}{4}$ in. diam) Te single-crystal rod. Te single crystals grow with the c axis [0001] along the axis of the hexagonal-faced crystal rod. Prism faces parallel to the c axis are known to be cleavage planes and lie along the $[10\bar{1}0]$ direction. Thin platelets along the [0001], $[10\bar{1}0]$, and $[2\bar{1}\bar{1}0]$ axes were spark cut after orienting the crystal rod along these different axes to better than $\frac{1}{2}^\circ$ of arc by the Laue back-reflection technique. After suitably supporting the single-crystal platelets, it was also possible, in some cases, to reduce the thickness of the platelets to 40–50 μ by spark planing. To make certain that spark planing of single-crystal absorbers did not cause surface damage, and, further, that a crystallographic phase change did not occur at

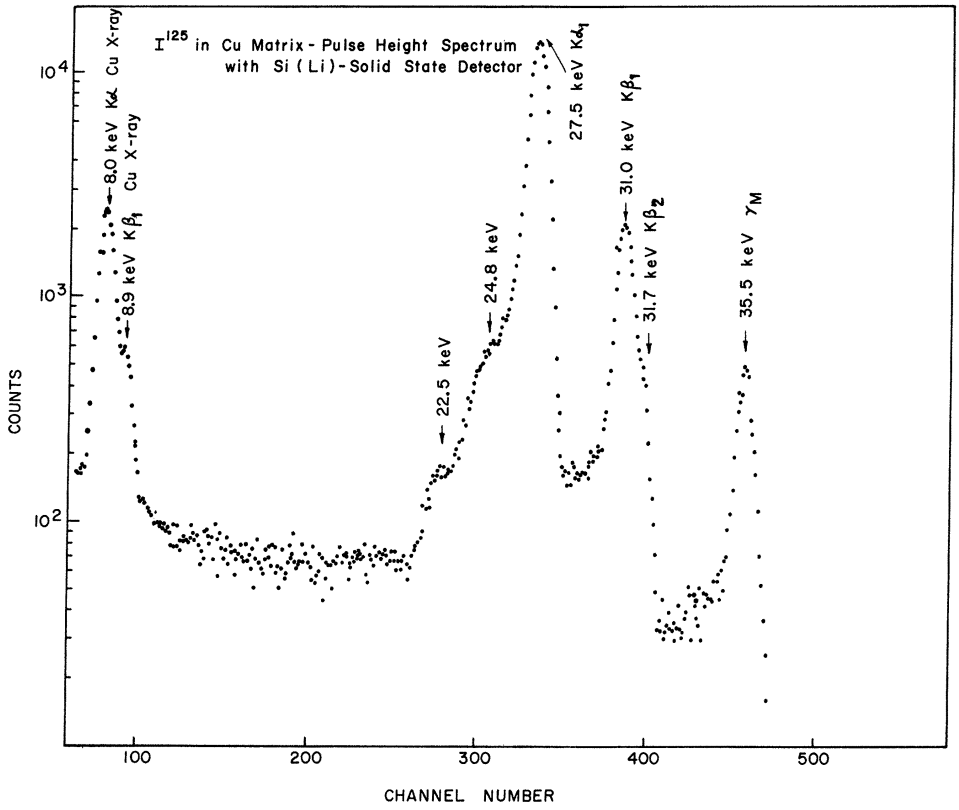

FIG. 1. Pulse-height spectrum of γ rays from I^{125} source in Cu-metal matrix, taken with Si(Li) detector.

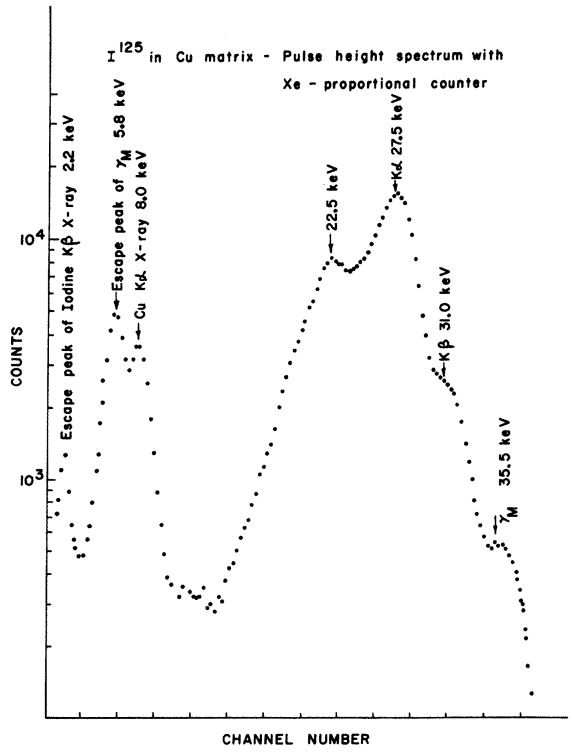

FIG. 2. Pulse-height spectrum of γ rays from I^{125} source in Cu-metal matrix, taken with Xe proportional count.

liquid-helium temperature, Laue back-reflection patterns were also taken after the experiments. An angular collimation of the γ rays received at the detector was of the order of 5° of arc.

III. EXPERIMENTAL RESULTS

Mössbauer spectra were taken with polycrystalline and single-crystal absorbers. The Te polycrystalline data (Fig. 4) showed a $(4 \pm 1)\%$ integral anisotropy of the quadrupole component. We believe that the origin of this anisotropy is the Karyagin-Goldanskii effect, arising from the spatial anisotropy of the recoilless fraction in Te metal.

The single-crystal data for γ-ray propogation parallel to the [0001] axis of Te were taken as a function of single-crystal absorber thickness. A total of four thicknesses (ranging from 40 to 400 microns) were used. Along the [0001] axis, the area under the lower-energy quadrupole component was found to be larger and a decrease in the anisotropy was observed with increasing absorber thickness (Figs. 5, 6). Figure 7 reproduces some of the single-crystal data taken from γ-ray propagation parallel to $[10\bar{1}0]$ and $[2\bar{1}\bar{1}0]$ axes. These data are reproduced in Table I. Along these directions perpendicular to the c axis, the anisotropy of the doublet was reversed; in other words, the area under the higher-energy quadrupole component was found to be larger. Analysis of the experimental

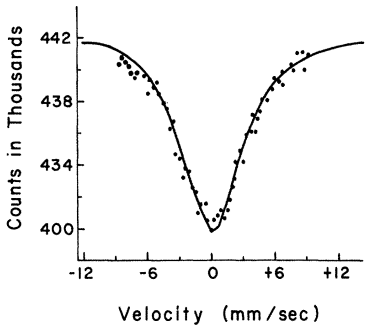

FIG. 3. Mössbauer spectrum with polycrystalline ZnTe absorber (3 mg/cm^2 of Te^{125}) at the temperature of liquid nitrogen. Each division on the x axis represents ten channels.

data to extract the ratio of the areas under the quadrupole doublet was carried out by a least-squares fit to two ideal Lorentzian lines with no restrictions on the line positions, intensities, and geometrical parameters. Because of the thinness of the absorbers, interference effects arising from the use of single crystals for the partially resolved quadrupole components were ignored.

IV. CRYSTAL STRUCTURE OF TELLURIUM

Tellurium belongs to the trigonal space group D_3^6 or D_3^4 (Fig. 8).[1,13] The crystallographic c axis is a threefold screw axis and there are three twofold axes in a plane normal to the trigonal axis. Looking along the c axis, the lattice consists of parallel spiral chains, each spiral possessing three atoms per turn with corresponding atoms of each spiral forming a hexagonal net. The lattice parameters and location of the three equivalent Te sites in the unit cell reported by Wyckoff are as follows:

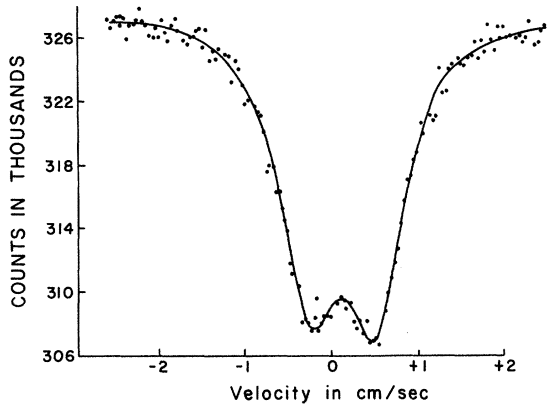

FIG. 4. Mössbauer spectrum with polycrystalline Te-metal absorber (3 mg/cm^2 of Te^{125}) at the temperature of liquid helium.

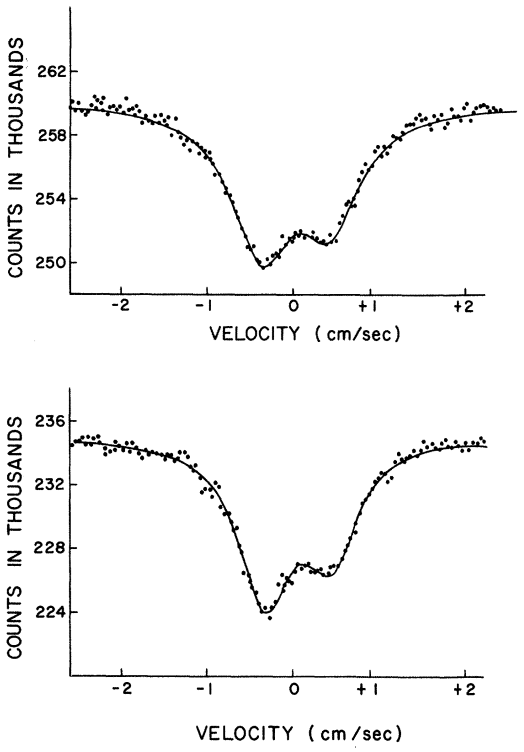

FIG. 5. Mössbauer spectra with Te-metal single crystals for the propagation of γ rays parallel to [0001] axis. The upper and the lower curves are for the crystal thicknesses of (120 ± 15) and $(40 \pm 15)\,\mu$, respectively.

Te $x, 0, 0,\ \bar{x}, \bar{x}, \frac{1}{3},\ 0, x, \frac{2}{3}$; $x = 0.269$,

$a = 4.447$ Å, $c = 5.915$ Å.

Figure 9 shows the Te coordinations which consist of two nearest-neighbor Te sites in the same chains, four second nearest neighbors in adjacent chains and six third nearest neighbors in adjacent chains. The bond lengths of nearest-neighbor sites (2.86 Å) and next-nearest-neighbor sites (3.45 Å) suggest that the bonding in a chain is strongly covalent in character and that between the chains it is relatively weaker.[14]

V. ANALYSIS AND RESULTS

The theoretical procedure for obtaining area ratios of the quadrupole doublet has been laid down by the works of Lang,[15] Zory,[10] and Housley.[14] The present case of Te metal becomes considerably involved for the following two reasons. In the first place, the crystal structure of Te permits three equivalent Te sites in the unit cell. Since, in a Mössbauer experiment, one observes the sum of the contributions due to the three sites, a sum over the angular part of the nuclear-resonance absorption cross section $P_\pi(\theta\phi)$ and $P_\sigma(\theta\phi)$ for the three sites is necessitated. Second, for the thick-

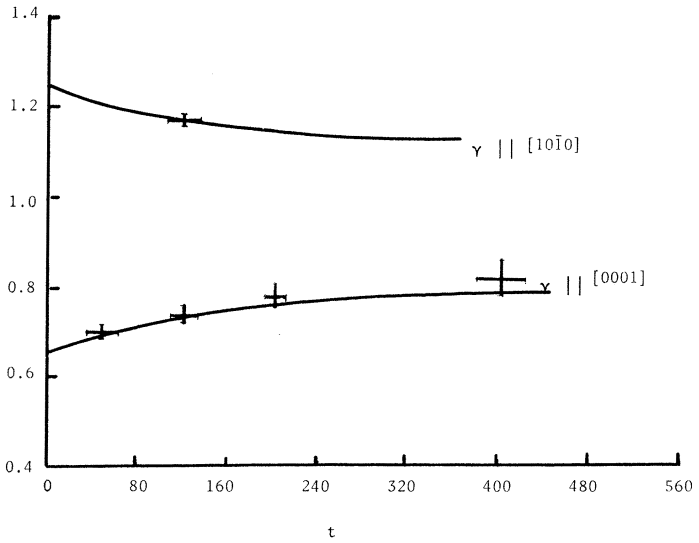

FIG. 6. Ratio I_π / I_σ plotted as a function of the thickness t (in μ) of the single-crystal absorbers.

ness of single-crystal absorbers used, the use of the thin-absorber approximation is not entirely justified. For absorbers which are not thin, additional parameters such as the principal values of the MSD tensor, Euler angles describing the orientation of the principal-axes system (PAS) of the MSD tensor, and polarization considerations enter into the theoretical area ratios. It is, however, possible to draw meaningful conclusions about the EFG and MSD tensors by restricting measurements along specific crystal axes and using arguments pertaining to the crystal symmetry to perform a self-consistent area-ratio analysis.

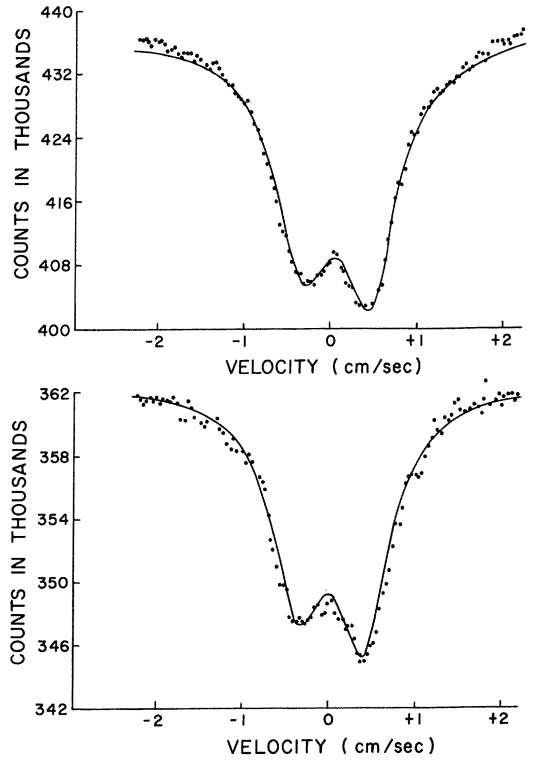

FIG. 7. Mössbauer spectra with Te-metal single crystals: upper curve is for propagation of γ rays along [10$\bar{1}$0] and lower curve is for propogation of γ rays along [2$\bar{1}\bar{1}$0]. In each case, the thickness of the Te-metal single crystal was (120 ± 15) μ.

A. γ-Ray Propagation Parallel to [0001] Axis

In a recent paper, [14] Housley *et al.* have worked out the restrictions placed on the index-of-refraction matrix from crystal symmetry considerations. For γ-ray propagation along a threefold screw axis, the index of refraction becomes diagonal in a system of right- and left-handed circular basis polarizations. Following the notation of Ref. 14, it follows that along the [0001] axis, the most general expression for the area ratios of the quadrupole doublet becomes

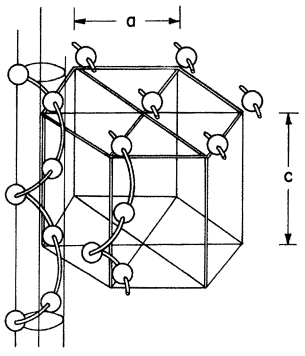

FIG. 8. Crystal structure of Te-metal lattice, Ref. 15.

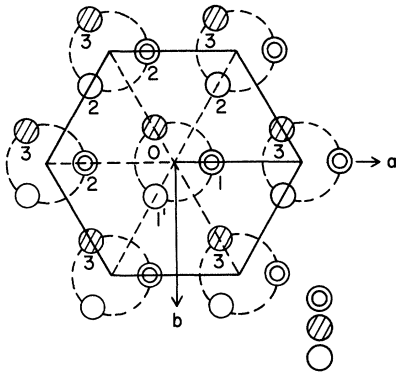

FIG. 9. Tellurium coordination (view along [0001] axis). The double circle represents the Te atomic site in the plane of the paper. The hatched circle represents Te atomic site above the plane of the paper at a distance $\frac{1}{3}c$ along the screw axis. The empty circle represents the Te atomic site above the plane of the paper at a distance $\frac{2}{3}c$ along the screw axis.

$$\frac{I_\pi}{I_\sigma}=\frac{\frac{1}{2}C_\pi e^{-C_\pi/2}\left[I_0(\frac{1}{2}C_\pi)+I_1(\frac{1}{2}C_\pi)\right]}{\frac{1}{2}C_\sigma e^{-C\sigma/2}\left[I_0(\frac{1}{2}C_\sigma)+I_1(\frac{1}{2}C_\sigma)\right]}\ , \tag{1a}$$

where

$$\begin{Bmatrix}C_\pi\\C_\sigma\end{Bmatrix}=n\sigma_0\sum_{\substack{i=1,2,3\\ \text{equivalent sites}}}\begin{Bmatrix}P_\pi(\theta_i\phi_i)\\P_\sigma(\theta_i\phi_i)\end{Bmatrix}f(\theta_i'\phi_i')\,, \tag{1b}$$

$$\begin{Bmatrix}P_\pi(\theta_i\phi_i)\\P_\sigma(\theta_i\phi_i)\end{Bmatrix}=\tfrac{1}{2}\pm\tfrac{1}{8}(1+\tfrac{1}{3}\eta^2)^{-1/2}\times(3\cos^2\theta_i-1+\eta\sin^2\theta_i\cos^2\phi_i)\,. \tag{1c}$$

Assuming the harmonic approximation for the recoilless fraction, one can write

$$f(\theta_i'\phi_i')=e-(1/\lambda^2)\left[\langle x^2\rangle\sin^2\theta_i'\cos^2\phi_i'+\langle y^2\rangle\sin^2\theta_i'\sin^2\phi_i'+\langle z^2\rangle\cos^2\theta_i'\right]. \tag{1d}$$

Here, $(\theta_i\phi_i)$ and $(\theta_i'\phi_i')$ designate the polar and azimuthal angles made by the γ-ray propagation vector $\vec{k}$ with respect to the PAS of the EFG tensor and MSD tensor, respectively. I_0 and I_1 denote Bessel functions of the zeroth and first order of imaginary arguments; and $\langle x^2\rangle$, $\langle y^2\rangle$, and $\langle z^2\rangle$ are components of the MSD tensor along its principal axis.

1. *Principle Axis of* EFG

The point-group symmetry P_{321} of Te requires one of the principal axes of the EFG to lie along the twofold axis passing through a given site. For Te, which possesses a partially filled p valence shell, it is well known[16] that the principal contribution to the EFG arises from the unbalanced p-electron density. This implies an overwhelming importance for the covalent bonds with the two nearest neighbors. An estimate of the fractional importance of this bond, by comparison with the case of iodine, has been placed close to 90%.[2,3] The nearest-neighbor approximation is then likely to be a good one for the case of Te. In this approximation, it is in fact possible to identify uniquely the other two principal axes of the EFG.

Since a given Te site forms two identical bonds with its two equidistant neighbors, a resonance of the covalent bond between the two equivalent molecular partners will occur. This is familiarly known as bond switching and was first proposed by Kojima *et al.*[17] It has been shown that on the assumption of bond switching, the EFG at a given site due to its two nearest neighbors acquires a diagonal form in the coordinate system shown in Fig. 10. In what follows, we shall assume the PAS of the EFG to be this one at respective sites.[3] It must, however, be emphasized that our approach in making such an assumption is to evolve a self-consistent solution to the problem. It has been shown[17] that if an axially symmetric Te – Te bond participates in the bond-switching mechanism, then the asymmetry parameter of the EFG is $\eta=3\cos\theta$, where θ is the Te – Te – Te bond angle. For the known angle $\theta=102.6°$, η worked out to be 0.65. For evaluating area ratios of the quadrupole doublet in the thin-absorber approximation ($C_\pi, C_\sigma \ll 1$), it can be readily seen that Eq. (1a) reduces to

$$\frac{I_\pi}{I_\sigma}=\frac{n\sigma_0\sum_i P_\pi(\theta_i\phi_i)f(\theta_i'\phi_i')}{n\sigma_0\sum_i P_\sigma(\theta_i\phi_i)f(\theta_i'\phi_i')}\ . \tag{2}$$

Let us consider first the case of the isotropic Debye-Waller factor. For this case, Eq. (2) reduces to

$$\frac{I_\pi}{I_\sigma}=\frac{\sum_i P_\pi(\theta_i\phi_i)}{\sum_i P_\sigma(\theta_i\phi_i)}\ . \tag{3}$$

In order to perform the sum over the three equivalent Te sites, a linear transformation from the PAS of the EFG to a crystal set of axes must be considered. The orthogonal crystal set of axes chosen for this purpose has been labeled a, b, and

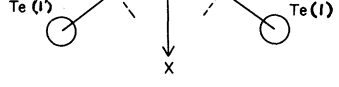

FIG. 10. Principal-axis system (PAS) of the electric field gradient (EFG) at $Te^{(0)}$ site.

TABLE I. Single-crystal data taken from γ-ray propagation.

Absorber thickness	I_π/I_σ
γ rays parallel to [0001] axis	
$52 \pm 15\ \mu$	0.70 ± 0.01
$120 \pm 15\ \mu$	0.74 ± 0.02
$200 \pm 15\ \mu$	0.78 ± 0.02
$400 \pm 15\ \mu$	0.82 ± 0.035
γ rays parallel to $[10\bar{1}0]$ axis	
$120 \pm 15\ \mu$	1.17 ± 0.01
γ rays parallel to $[2\bar{1}\bar{1}0]$ axis	
$120 \pm 15\ \mu$	1.16 ± 0.01

c, with the c axis of the orthogonal set along the [0001] axis and the a axis along the $[2\bar{1}\bar{1}0]$ axis of Te. The following transformation essentially allows one to go from a $\theta_i\phi_i$ basis to a $\theta\Phi$ (Fig. 11):

$$\begin{pmatrix} \sin\theta_i\cos\phi_i \\ \sin\theta_i\cos\phi_i \\ \cos\theta_i \end{pmatrix} = \begin{pmatrix} X_{ai} & X_{bi} & X_{ci} \\ Y_{ai} & Y_{bi} & Y_{ci} \\ Z_{ai} & Z_{bi} & Z_{ci} \end{pmatrix} \begin{pmatrix} \sin\theta\cos\Phi \\ \sin\theta\sin\Phi \\ \cos\theta \end{pmatrix} .$$

X_{ai}, X_{bi}, X_{ci}, etc. define the direction cosines of XYZ principal axes of the EFG with respect to the crystal set of axes in which measurements are made. From the known crystal structure of Te and some solid-geometry considerations, the direction cosines of the three PAS's of the EFG with respect to the crystal set of axes were calculated and the results are summarized in the Appendix. With the help of these direction cosines the right-hand side of Eq. (3) can be computed with η as parameter. This gives

$$\frac{I_\pi}{I_\sigma} = \frac{\sum_i \{\frac{1}{2} + \frac{1}{8}(1+\frac{1}{3}\eta^2)^{-1/2}[(\eta-1)+(3-\eta)Z_{ci}^2 - 2\eta Y_{ci}^2]\}}{\sum_i \{\frac{1}{2} - \frac{1}{8}(1+\frac{1}{3}\eta^2)^{-1/2}[(\eta-1)+(3-\eta)Z_{ci}^2 - 2\eta Y_{ci}^2]\}} , \tag{4}$$

$$\frac{I_\pi}{I_\sigma} = \frac{1.5 - \frac{1}{8}(1+\frac{1}{3}\eta^2)^{-1/2}(1.05+2.35\eta)}{1.5 + \frac{1}{8}(1+\frac{1}{3}\eta^2)^{-1/2}(1.05+2.35\eta)} . \tag{5}$$

Figure 12 shows a plot of Eq. (5) with η as a variable parameter over the interval 0 to 1. It is interesting to note that along the [0001] axis the intensity of the σ component is always larger than the π component. This point is discussed in detail in Sec. VI. This at once leads to the conclusion that the higher-energy component in the quadrupole spectrum is the π component. The quadrupole interaction in Te metal is thus positive. From the known quadrupole moment of the 35.5-keV state of Te^{125} as $-(0.19 \pm 0.02)$ b, [18] the Z component of the EFG in Te metal is thus found to be negative and has a magnitude of $V_{zz} = (9.2 \pm 1.0) \times 10^{18}$ V/cm^2. [19]

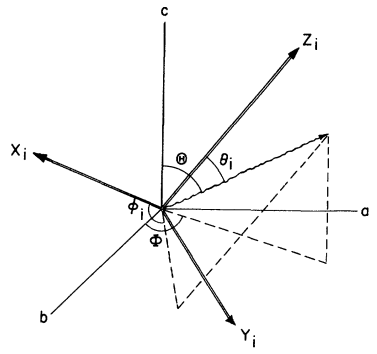

FIG. 11. Polar and azimuthal angle of the γ-ray propagation vector $\vec{k}$ with respect to the principal axis of the EFG (X_i, Y_i, Z_i,) and the crystal site of axes ($a, b, c,$).

2. PAS *of* MSD

The point group of Te requires one of the principal axes of the MSD tensor to lie along the twofold axis passing through a given site, but lays no restriction on the possible choice of the other two principal axes. In view of a rather well-defined symmetry about the Te site in the metal structure,

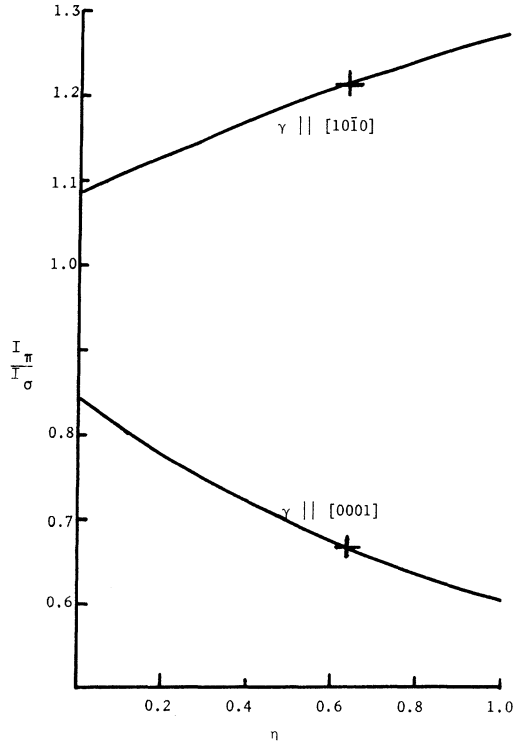

FIG. 12. Ratio I_π/I_σ as a function of the asymmetry parameter η in the thin absorber approximation.

in what follows, we shall assume that the PAS of the EFG and MSD coincide.

One can now evaluate in a rather straightforward way I_π/I_σ as a function of absorber thickness for γ ray parallel to the [0001] axis, once the PAS of the two tensors are known. From the definition of

$$\begin{Bmatrix} C_\pi \\ C_\sigma \end{Bmatrix}$$

given in Eq. (1a), it follows that

$$\begin{Bmatrix} C_\pi \\ C_\sigma \end{Bmatrix} = n\sigma_0 \sum_i \{[\tfrac{1}{2} \pm \tfrac{1}{8}(1+\tfrac{1}{3}\eta^2)^{-1/2} \times [(\eta-1)+(3-\eta)Z_{ci}{}^2 - 2\eta Y_{ci}{}^2]\} \times \exp[-(\langle y^2\rangle Y_{ci}^2 + \langle z^2\rangle Z_{ci}^2)/\lambda^2] \ . \quad (6)$$

Fortunately, the values of Z_{ci}^2 and Y_{ci}^2 are the same for all the three sites; consequently, the sum is readily performed:

$$\begin{Bmatrix} C_\pi \\ C_\sigma \end{Bmatrix} = n\sigma_0 [1.5 + \tfrac{3}{8}(1+\tfrac{1}{3}\eta^2)^{-1/2} \times [(\eta-1)+(3-\eta)Z_{ci}^2 - 2\eta Y_{ci}^2]\} \times \exp[-(\langle y^2\rangle Y_{ci}^2 + \langle z^2\rangle Z_{ci}^2)/\lambda^2] \ . \quad (7)$$

The behavior of I_π/I_σ against η is not sensitive to small anisotropies in the Debye-Waller factor.[20]

A linear extrapolation procedure for obtaining I_π/I_σ for zero absorber thickness from the experimental data yields a value for the asymmetry parameter η which is indeed quite close to the value of 0.65 (Fig. 12). The final theoretical fit to the experimental data along this axis was obtained by using Eq. (6) to obtain

$$\begin{Bmatrix} C_\pi \\ C_\sigma \end{Bmatrix}$$

to solve Eq. (10) as a function of $\langle y^2\rangle/\lambda^2$, $\langle z^2\rangle/\lambda^2$, and η. For the appropriate range of values of $\langle y^2\rangle/\lambda^2$, $\langle z^2\rangle/\lambda^2$, and η, a family of curves of I_π/I_σ against absorber thickness[12] was obtained. The values of σ_0 and α_T were taken from Ref. 12. The parameter η basically determines the intercept of these curves on the abscissa; the MSD parameters $\langle y^2\rangle$ and $\langle z^2\rangle$ determine the way these curves saturate as a function of thickness. The analysis of the data is not sensitive to individual values of $\langle y^2\rangle/\lambda^2$ and $\langle z^2\rangle/\lambda^2$ but rather to the sum of their values [Eq. (6)]. Since we have no *a priori* information on these principal values of the MSD, $\langle y^2\rangle$ was taken equal to $\langle z^2\rangle$. Our best fit to the experimental data along this axis gave us

$$\eta = 0.64 \pm 0.04, \quad \langle y^2\rangle = \langle z^2\rangle = (1.6 \pm 0.05)\lambda^2 \ ,$$

$$f_c = (0.60 \pm 0.03), \quad \Theta_D = (180 \pm 20)\,^\circ\mathrm{K} \ .$$

No correction to the area ratios I_π/I_σ was made for the finite angular spread in collimation of γ rays detected in the transmission geometry. Presumably, such a correction would have the effect of increasing the anisotropy, and correspondingly increasing the values of the MSD parameters. The fit was actually obtained to correspond to the minimum value of the recoilless fraction permissible within the experimental uncertainties. The Debye temperature of tellurium metal is reported to be 129 (Ref. 21) and 153 °K (Ref. 22) found by other techniques.

B. γ-Ray Propagation Parallel to [1010] Axis

For γ-ray propagation perpendicular to a twofold axis, the index-of-refraction matrix acquires a diagonal form in a basis of linear polarization parallel and normal to the symmetry axis. Along such a direction, the area ratios of the quadrupole component are, in general, polarization dependent and a calculation of fractional polarization a_π and a_σ[23] becomes necessary. For the present case of Te where there are three equivalent sites in the unit cell, calculations for a_π and a_σ become a little tedious, although, in principle, the procedure has been well laid out.[15] In order to be able to sum the polarization-density matrices of all sites, one has to transform to a common basis the 2×2 polarization-density matrices

$$\begin{pmatrix} \rho_{11} & \rho_{12} \\ \rho_{21} & \rho_{22} \end{pmatrix}$$

associated with each site. The matrices are defined in the PAS of the EFG at each site. The crystal set of axes *abc* was used as a common basis for this purpose. A similarity transformation of the 2×2 polarization-density matrix from the EFG PAS to the crystal set of axes was done with the help of Cayley-Klein parameters.[24] The Cayley-Klein parameters associated with transformation from a given site i can be obtained directly once the direction cosines associated with the isomorphic 3×3 transformation matrix are known. Results of calculations indicate that for $\eta = 0.64$, the fractional polarization a_π and a_σ are quite small and are equal to 0.01 and 0.04, respectively. This may not be surprising if one considers the fact that one is dealing here with a crystal structure where in fact an averaging process is already built into the unit cell. Thus, polarization effects do not play an important role in determining the area ratios along this direction and will be ignored in what is to follow. We have used Eq. (1) to obtain I_π/I_σ as a function of absorber thickness along this direction. In the limit of zero absorber thickness, I_π/I_σ is a function of η alone. It is a straightforward calculation to show, using Eq. (3), that for γ rays parallel to $[10\bar{1}0]$,

$$\frac{I_\pi}{I_\sigma} = \frac{1.5 + \frac{1}{8}(1+\frac{1}{3}\eta^2)^{-1/2}(1.77\eta + 0.525)}{1.5 - \frac{1}{8}(1+\frac{1}{3}\eta^2)^{-1/2}(1.77\eta + 0.525)} \quad ; \qquad (8)$$

Eq. (8) describes the behavior of I_π/I_σ as a function of η. A plot of Eq. (8) is given in Fig. 12. It is interesting to note that along this direction I_π/I_σ is always greater than 1 over the possible domain of η and, in particular, for $\eta = 0.64$, $I_\pi/I_\sigma = 1.22$. The fit to the experimental data along this direction was obtained by keeping $\langle x^2\rangle/\lambda^2$ as the only variable parameter, the other parameters, namely, y^2/λ^2 and z^2/λ^2 being fixed to their values obtained from the analysis along the [0001] axis. This gave a value of

$$\langle x^2\rangle = (1.6 \pm 0.05)\lambda^2 .$$

The Debye temperature for γ-ray propagation perpendicular to the c axix is found equal to 180 ± 15 °K. In the course of this investigation, the quadrupole splitting of Te metal was measured ten times at liquid-helium temperature, and an average of all runs gave

$$\Delta E_q = (7.74 \pm 0.10) \text{ mm/sec} .$$

This value is in agreement with previous measurements.[2,3]

VI. DISCUSSION

The area analysis provides a description of the EFG and MSD parameters for Te metal. We find that the experimental data can be explained on the basis of a collinear PAS for the two tensors. Physically, such a result can be understood from the fact that the Te site possesses a well-defined P_{321} symmetry where the role of nearest neighbors is dominant. From the radiation patterns of the π and σ quadrupole components, it is well known that along the z axis of the EFG, the π component is in general enhanced, and furthermore, in a direction normal to the z axis of the gradient, the σ component is enhanced. Qualitatively speaking, from our results obtained along the [0001] axis of Te, which is a direction more perpendicular than parallel to the z axis of the gradients (Appendix) at the three sites, one can understand the enhancement of the π quadrupole component in the Mössbauer spectrum. Likewise, along the $[10\bar{1}0]$ axis of tellurium, which is a direction almost parallel to the z axis of the gradients (Appendix) at the three Te sites, an enhancement of the π quadrupole component in the Mössbauer spectrum is also understood.

The value of 0.64 ± 0.04 [2,3] obtained for the asymmetry parameter clearly suggests that the nearest-neighbor approximation for the electric quadrupole interaction in Te metal is indeed a good one. The actual EFG PAS at a given site falls close to the one determined by nearest neighbors only. The result also reflects on the fact that the intramolecular Te – Te bond in the solid state is axially symmetric.

Pasternak and Bukhspan[18] using ME studies in I^{129}, have investigated the electric hyperfine field at an iodine impurity in a Te-metal host. Their results at liquid-nitrogen temperature indicate a quadrupole interaction of 532 ± 10 MHz and an asymmetry parameter $\eta = 0.80 \pm 0.05$. The iodine impurity experiences an EFG which has a lower magnitude V_{zz} and is described by a larger asymmetry parameter than does a regular Te site in the same Te-metal host. We feel that a comparison of the results obtained in the two measurements is not entirely valid. First, the two measurements have been made at different temperatures; second, and rather more important, one does not have any specific knowledge of the location of the iodine impurity site in Te metal. In fact, from the available information it appears likely, as suggested by Pasternak, that the iodine impurity does not substitute the Te site in the Te-metal lattice. It would be interesting to perform the I^{129} experiment at liquid-helium temperature to be able to compare results at the same temperature.

The analysis also reveals that the MSD parameters $\langle y^2\rangle/\lambda^2$ and $\langle z^2\rangle/\lambda^2$ cannot be independently obtained with precision. If one assumes $\langle y^2\rangle = \langle z^2\rangle$, then we find that a fit to the experimental data along and perpendicular to the c axis gives the Debye temperature $\Theta_D = (180 \pm 20$ °K). In the limits of our experimental uncertainties the recoilless fraction is found to be isotropic.

When the quadrupole doublet is not completely resolved, accurate values of area ratios I_π/I_σ become difficult to achieve. It may, however, be possible to improve on the statistical uncertainties of the present experiment by using a better-quality single-line source. I^{125} in a Cu matrix does not give the natural width, and furthermore the Debye temperature of the source leaves much to be desired.

ACKNOWLEDGMENTS

We are indebted to Dr. R. M. Housley of the North American Aviation Center for some valuable correspondence on the polarization considerations in single-crystal experiments. Dr. D. M. Sparlin gave valuable advice on some experimental problems. Discussions with Professor Benjamin Segall, Professor Bernard Goodman, and Dr. Larry Campbell went a long way to clarify some concepts on polarization considerations. Charles Telesco, summer undergraduate research participant, was responsible for processing data.

APPENDIX

The direction cosines are

$$\begin{bmatrix} X_{ai} & X_{bi} & X_{ci} \\ Y_{ai} & Y_{bi} & Y_{ci} \\ Z_{ai} & Z_{bi} & Z_{ci} \end{bmatrix} ,$$

$$\begin{bmatrix} 1 & 0 & 0 \\ 0 & -2\beta & \gamma \\ 0 & \gamma & 2\beta \end{bmatrix} \text{ for } i=1,$$

$$\begin{bmatrix} -\frac{1}{2} & \sqrt{3}/\sqrt{2} & 0 \\ \beta\sqrt{3} & \beta & \gamma \\ \gamma\sqrt{3}/\sqrt{2} & \frac{1}{2}\gamma & -2\beta \end{bmatrix} \text{ for } i=2,$$

$$\begin{bmatrix} \frac{1}{2} & \sqrt{3}/\sqrt{2} & 0 \\ -\beta\sqrt{3} & \beta & \gamma \\ -\gamma\sqrt{3}/\sqrt{2} & \frac{1}{2}\gamma & -2\beta \end{bmatrix} \text{ for } i=3,$$

where

$$\beta = \tfrac{3}{2}\sqrt{3}ax/(27a^2x^2+4c^2)^{1/2},$$

$$\gamma = ax/(27a^2x^2+4c^2)^{1/2},$$

with a, x, and c having been defined in the text.

---

*From a dissertation submitted by P. Boolchand in partial fulfillment of the requirements for the degree of Doctor of Philosophy at Case Western Reserve University, 1969 (unpublished).

†Present address: University of Cincinnati, Cincinnati, Ohio 45221.

‡Present address: Education Research Center, Massachusetts Institute of Technology, Cambridge, Mass.

[1]R. W. G. Wyckoff, *Crystal Structures*, 2nd ed. (Interscience, New York, 1963).

[2]C. E. Violet, *Mössbauer Effect and Its Applications in Chemistry* (American Chemical Society, Washington, D. C., 1967), p. 147.

[3]C. E. Violet, R. Booth, and F. Wooten, Phys. Letters 5, 230 (1963).

[4]N. Shikazono, J. Phys. Soc. Japan 18, 925 (1963).

[5]C. E. Violet and R. Booth, Phys. Rev. 144, 225 (1966).

[6]G. Albanese, C. Lamborizio, and I. Ortalli, Nuovo Cimento 50B, 66 (1967).

[7]J. Danon and L. Iannarella, J. Chem. Phys. 47, 382 (1967).

[8]R. W. Grant, R. M. Housley, and U. Gonser, Phys. Rev. 178, 523 (1969).

[9]R. Ingalls, K. Ono, and L. Chandler, Phys. Rev. 172, 295 (1968).

[10]P. Zory, Phys. Rev. 140, A1401 (1965).

[11]M. Kalvius, in *Mössbauer Effect Methodology*, edited by I. J. Gruverman (Plenum, New York, 1965), Vol. 1, p. 177.

[12]A. H. Muir, K. J. Ando, and H. M. Coogan, *Mössbauer Effect Data Index* 1958–1965 (Interscience, New York, 1966).

[13]J. S. Blakemore, D. Long, K. C. Namura, and A. Nussbaum, *Progress in Semiconductors* (Wiley, New York, 1962), Vol. 6, p. 39.

[14]R. M. Housley, R. W. Grant, and U. Gonser, Phys. Rev. 178, 514 (1969).

[15]G. Lang, Nucl. Instr. Methods 24, 425 (1963).

[16]C. H. Townes and B. P. Dailey, J. Chem. Phys. 17, 782 (1949).

[17]S. Kojima, K. Tsukada, S. Ogawa, A. Schimauchi, and Y. Abe, J. Phys. Soc. Japan 9, 805 (1954).

[18]M. Pasternak and S. Bukhspan, Phys. Rev. 163, 297 (1967).

[19]P. Boolchand, B. L. Robinson, and S. Jha, Bull. Am. Phys. Soc. 1, 14 (1969). The values of η and V_{zz} quoted in the above reference were incorrect. The value of $\eta = 0.45 \pm 0.05$ was due to an incorrect analysis of the data and the value of V_{zz} was inadvertently quoted $(4.6 \pm 0.5) \times 10^{18}$ V/cm^2 which is a factor 2 less than what it should have been.

[20]V. I. Goldanskii, E. F. Makarov, I. P. Suzdalev, and I. A. Vinorgradov, Phys. Rev. Letters 20, 137 (1968).

[21]T. Fukuroi and Y. Muto, Sci. Rept. Res. Inst. Tohoku Univ. Ser. A 8, 213 (1956).

[22]P. L. Smith, Bull. Inst. Intern. Froid, Annexe 51, 281 (1959).

[23]R. M. Housley, U. Gonser, and R. W. Grant, Phys. Rev. Letters 20, 1279 (1968).

[24]H. Goldstein, *Classical Mechanics* (Addison-Wesley, Reading, Mass., 1959).